THE JOURNAL OF PHYSICAL CHEMISTRY Letters

Letter

pubs.acs.org/JPCL

$Ag_{44}(SeR)_{30}$: A Hollow Cage Silver Cluster with Selenolate Protection

Indranath Chakraborty,[†] Wataru Kurashige,[‡] Keita Kanehira,[‡] Lars Gell,[§] Hannu Häkkinen,[§] Yuichi Negishi,*[,‡] and Thalappil Pradeep*[,†]

[†]DST Unit of Nanoscience (DST UNS) and Thematic Unit of Excellence (TUE), Department of Chemistry, Indian Institute of Technology Madras, Chennai 600 036, India

[‡]Department of Applied Chemistry, Faculty of Science, Tokyo University of Science, 1-3 Kagurazaka, Shinjuku-ku, Tokyo 162-8601, Japan

[§]Departments of Chemistry and Physics, Nanoscience Center, University of Jyväskylä, Box 35, FI-40014 Jyväskylä, Finland

Supporting Information

ABSTRACT: Selenolate protected, stable and atomically precise, hollow silver cluster was synthesized using solid state as well as solution state routes. The optical absorption spectrum shows multiple and sharp features similar to the thiolated Ag_{44} cluster, $Ag_{44}(SR)_{30}$ whose experimental structure was reported recently. High-resolution electrospray ionization mass spectrometry (HRESI MS) shows well-defined molecular ion features with two, three, and four ions with isotopic resolution, due to $Ag_{44}(SePh)_{30}$. Additional characterization with diverse tools confirmed the composition. The closed-shell 18 electron superatom electronic structure, analogous to $Ag_{44}(SR)_{30}$ stabilizes the dodecahedral cage with a large HOMO−LUMO gap of 0.71 eV. The time-dependent density functional theory (TDDFT) prediction of the optical absorption spectrum, assuming the $Ag_{44}(SR)_{30}$ structure, matches the experimental data, confirming the structure.

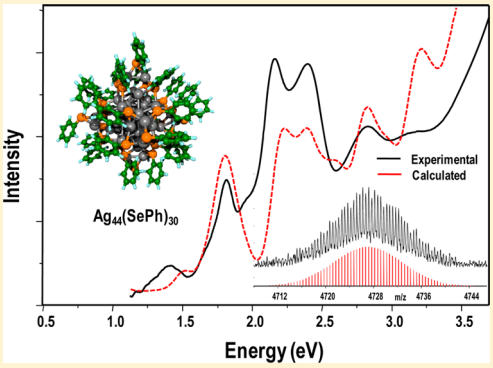

SECTION: Physical Processes in Nanomaterials and Nanostructures

Noble metal nanoparticles[1−4] and their atomically precise analogues,[5−7] called by various names (artificial atoms, nanomolecules, and quantum clusters), due to their diverse and technologically relevant properties have had a profound impact on the science of nanosystems.[8−16] Nearly all of these systems have been prepared with thiols[8,11,15,17−19] as their protecting agents, although phosphines have been the preferred ligands in the early period of this science.[20−24] Accurate structures of some of the thiolated clusters are now available in the literature.[25−30] Most of these pertain to gold and the first crystal structures of silver analogues[31,32] have just appeared. Many other silver clusters have been identified by mass spectrometry.[33−36] The most recent $Ag_{44}(SR)_{30}$ system forms a Keplerate solid of concentric icosahedral and dodecahedral atom shells, which are further protected by six $Ag_2(SR)_5$ units in an octahedral geometry, as revealed from single crystal studies.[37,38] It is the first hollow cage system of a noble metal cluster to have been crystallized with thiolate protection although a cage structure has been predicted for $Au_{144}(SR)_{60}$[39] and more recently for $Ag_{152}(SR)_{60}$.[40]

In this Letter, we report the $Ag_{44}(SePh)_{30}$ (**1**) system, the very first selenolate analogue of a silver cluster with nearly identical properties of the thiolate system. Examples of selenolate protected clusters are very few in the literature; those available are on gold and show higher stability compared to the thiolate analogues.[41−44] However, selenolate protected silver nanoparticles have been reported by Zaluzhna et al.[45] The homologous family of $Ag_{44}(XR)_{30}$ system[37,38,46−48] (X = S, Se) and their unique properties with molecule-like optical absorption, high stability, easy synthesis, and potential to scale up are expected to attract immediate attention of the scientific community. Density functional theory (DFT) calculations reveal that the exceptional stability of the cluster can be traced back to a strong electronic shell closing at 18 electrons similar to the reported case of the $Ag_{44}(SR)_{30}^{4-}$ cluster[38] and time-dependent DFT (TDDFT) calculations of $Ag_{44}(SePh)_{30}^{4-}$ based on the reported structure of the thiolate analog predict an optical absorption spectrum in complete agreement with the experiment.

$Ag_{44}(SePh)_{30}$ (**1**) was made initially via a solid state method originally reported for the $Ag_9(SR)_7$ system, with significant modifications (see the Experimental Methods section for details).[49] Solid state reaction conducted in a mortar and pestle under ambient atmospheric condition results in a series of color changes (photographs are given in Figure S1). In the solid state route, the cluster growth is controlled by the limited supply of water needed for the reduction of silver thiolate by $NaBH_4$ (s), which becomes available from the laboratory atmosphere as well as from the ethanol used for subsequent washing.[40] The cluster appeared deep pink (inset of Figure 1)

Received: September 3, 2013
Accepted: September 20, 2013

   dx.doi.org/10.1021/jz401879c | J. Phys. Chem. Lett. 2013, 4, 3351−3355

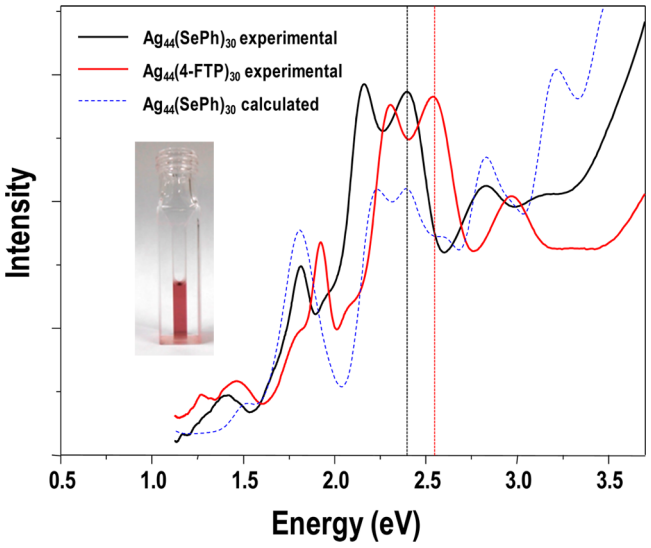

Figure 1. The optical absorption spectra for cluster **1** (black trace) and **2** (red trace), respectively, in acetone and THF solvent, plotted in terms of energy. Dashed blue line shows the corresponding calculated optical absorption spectrum of cluster **1**. The individual optical transitions in the calculated spectrum are broadened by 0.05 eV Gaussians, and the intensity is scaled to match with the experimental spectrum; details are given in the Supporting Information. The spectrum reveals multiple maxima with five prominent bands and three broad bands. The computed spectral features are matching very well with cluster **1**. The red shift in the Se analogue, shown with vertical lines originates from a simple size effect as discussed in the text. Inset shows the photograph of cluster **1** solution in acetone, taken in a cuvette.

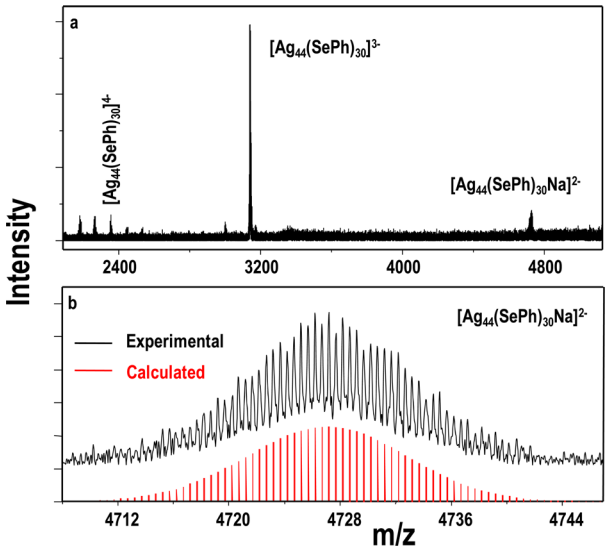

Figure 2. (a) HRESI MS of as-synthesized cluster **1** taken in negative mode. The spectrum shows clear 2-, 3- and 4-ions of the $Ag_{44}(SePh)_{30}$. Clean spectrum suggests the purity of the as-synthesized cluster. Sodium exists as the counterion. (b) Expanded mass spectrum of the 2-ion (black traces). Spectrum is matching exactly with the calculated one (red trace).

in acetone/acetonitrile that was stored at 4 °C in a refrigerator. The yield was 80%. It is important to note that at room temperature (25 °C) and atmospheric conditions, the cluster degrades in 15 days forming yellow Ag-selenolates. However, stability is of the order of months in the solid state in the refrigerator. We have also used a solution phase route to make the clusters, a modified version of the process used to make $Ag_{44}SR_{30}$.[47] The corresponding thiolated cluster, $Ag_{44}(4\text{-FTP})_{30}$ (FTP = 4-Fluorothiophenol) (**2**) was also prepared for comparison.[47,48] Details of experimental procedures and characterization methods including density functional computations are given in the Supporting Information.

The optical absorption spectrum of **1** (black trace in Figure 1 and S2Aa) shows characteristic features in the 300 to 900 nm region. Five intense bands at 1.41(879), 1.82 (681), 2.16 (574), 2.40 (516) and 2.82 (440) eV (nm) along with three broad bands centered around 1.27 (970), 1.95 (635) and 3.14 (395) eV (nm) were seen. Interestingly, the spectral features are matching with the corresponding thiolated Ag_{44} cluster **2** (red trace in Figure 1 and S2Ab) identified by Harkness et al.[48] However, some red shift is seen, attributed to a size effect as discussed later. Here, it may be noted that the ligand does not contain substituents on the phenyl ring, which would modify the electron density. The profound similarity of the spectrum with that of cluster **2** made us explore its properties in greater detail. The cluster synthesized through the solution phase shows similar features in the optical absorption spectra as the cluster made through the solid state. Comparative spectra for both are given in Figure S2B. The time-dependent data for the cluster synthesized through solid (Figure S3A) and solution (Figure S3B) state routes show increased stability of the samples under ambient conditions.

Further confirmation of the composition comes from mass spectrometry. Electrospray ionization mass spectrometry gave sharp and distinct 4-, 3-, and 2- features of $Ag_{44}(SePh)_{30}$ and the spectrum reveals $Ag_{44}(SePh)_{30}$ as an integral species (Figure 2a). The 2- feature shows a series of closely spaced peaks centered at m/z 4727.5 with a width of ±12, due to the characteristic isotope distribution which matches well with the calculated pattern. The experimental and calculated spectra are compared in Figure 2b. It is important to note that Se has six isotopes and in conjunction with the two isotopes of silver with equal abundance, peaks in the 4- and 3- regions are complex. Sodium exists as a countercation with the cluster. Despite these complexities, expanded spectrum in the 3- charge state clearly shows the isotope resolution (Figure S4). The 4- feature is weak and, consequently, the isotope resolution is unclear (Figure S4). The reason behind higher intensity of 3- compared to 4- is unknown, but it is important to note here that the intensity also depends on instrument parameters. We optimized the conditions to achieve the best isotope resolution, irrespective of relative intensity. Although a 4- ion is seen, we note that ESI MS does not confirm the existence of this charge state in solution as additional ionization events can occur during electrospray. Even 5-, 6-, and 7- peaks are also observed for $Ag_{44}(SR)_{30}$.[46]

The mass spectrometric suggestion of the molecular formula was confirmed by various analytical measurements. Thermogravimetric (TG) analysis of **1** shows a single and sharp mass loss (at ~240 °C) of 48.38%, as expected (Figure 3a). Part of the counterion, sodium (as $Ag_{44}(SePh)_{30}$ is a 4- species, see below) may still be attached with the cluster at 550 °C, which leaves some uncertainty in calculating the exact % loss. The weight loss starts from ~200 °C, which is quite a high temperature compared to the most stable $Au_{25}(SeR)_{18}$ cluster,[41] suggesting high stability and rigidity of the cluster. A cluster core of 1.0 ± 0.2 nm was confirmed from TEM (Figure 3b),

dx.doi.org/10.1021/jz401879c | J. Phys. Chem. Lett. 2013, 4, 3351−3355

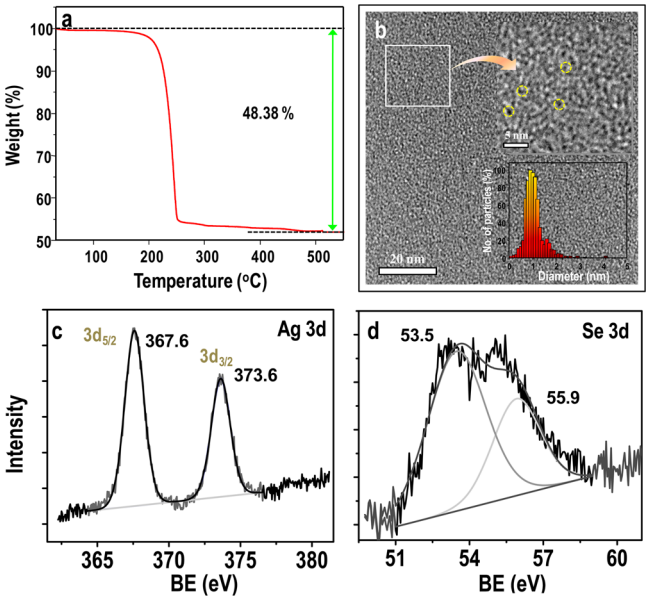

Figure 3. (a) TG analysis of cluster **1**. The spectrum shows a sharp loss at 240 °C. Mass loss started from ∼200 °C onward, suggesting high stability for the cluster. HRTEM image in b shows tiny particles and an expanded portion is given in the inset. Some particles are marked with yellow circles. Inset shows the size distribution. Narrow distribution suggests high uniformity of the cluster. Expanded XPS spectra of Ag 3d (c) and Se 3d (d). Peak positions are marked accordingly. The 55.9 eV feature in d is due to X-ray induced damage of the sample.

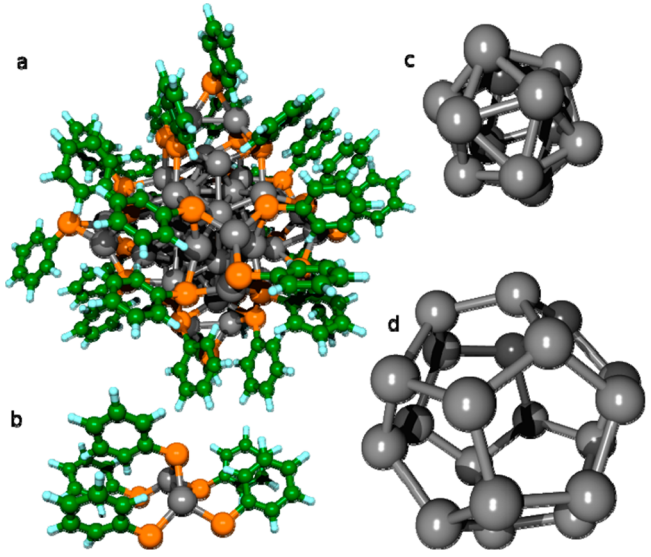

Figure 4. (a) Computationally relaxed structure of the $Ag_{44}(SePh)_{30}^{4-}$ cluster, showing in addition (b) the structure of one $Ag_2(SePh)_5$ surface unit and the (c) icosahedral and (d) dodecahedral shells of the metal core. Ag: gray; Se: orange; C: green; H: cyan.

which is quite similar to that reported for the $Ag_{44}(SR)_{30}$ cluster where the core size was found to be 1.3 nm. Uncertainty of the measurement at such small core sizes prevented us from getting a closer value. The narrow size distribution suggests uniformity of the cluster. Elemental analysis (Figure S5) showed an Ag:Se ratio (1:0.679) similar to that expected (1:0.682). Other expected elements are also seen in the spectrum. The loss of Se−H proton (at 3.5 ppm) was seen in ^{1}HNMR, which confirms the binding of silver with the selenolate species (Figure S6). Because of metal attachment to the ligand, the aromatic protons show downfield shift and they get broadened as expected.

XPS of **1** shows the expected elements in the predictable intensity pattern (Figure S7). Ag 3d appears at 367.6 eV, typical of metallic silver (Figure 3c). It is important to note that the difference between Ag(0) and Ag(I) is small (0.5 eV)[50] and a precise determination of the valence state is not possible with the available instrumental resolution. Se 3d appears at 53.5 eV as expected (Figure 3d) for the selenolate system.[43] However, as there is a possibility of X-ray induced damage, the Se 3d region shows an additional feature at 55.9 eV. This kind of X-ray-induced damage is seen in the thiolate system,[51] possibly due to the sulfate or sulfonate species, arising from X-ray exposure.

Motivated by the similarity of the measured optical spectra of $Ag_{44}(XR)_{30}$ (X = S, Se) clusters, we performed DFT computations of the electronic ground state and TDDFT computations on the optical spectrum (blue trace in Figure 1) of $Ag_{44}(SePh)_{30}^{4-}$ based on the resolved structure[38] of the thiolate analogue, $Ag_{44}(SPhF_2)_{30}^{4-}$ (for computational details, see Supporting Information). Very small but systematic expansion of the selenolate protected cluster as compared to the thiolate-analogue was observed in the DFT-optimized structure of (**1**) shown in Figure 4 (for comparison of important bond lengths, see S8 Table 1). These differences are mainly due to the slightly larger covalent/ionic radius of Se compared to S. The free electron count of the compound in the 4- charge state is 18, applying the simple electron counting rule of ref 52. This corresponds to the $1S^2$ $1P^6$ $1D^{10}$ superatom electron configuration, thus leaving the $2S^2$ and $1F^{14}$ manifolds empty (see Figure S9 showing the electronic density of states for the region of the superatom 1D, 2S, and 1F states). The destabilization of the $2S^2$ superatom state is due to the hollow cage structure of the inner metal core.

The calculated HOMO−LUMO gap is 0.71 eV showing the electronic stability. The HOMO−LUMO optical transition is, however, dipole-forbidden, and the optical gap is therefore slightly larger. The calculated optical absorption spectrum of $Ag_{44}(SeR)_{30}$ for charge state 4- matches with all the observed major features, thus indicating that the known structure of $Ag_{44}(SR)_{30}$ is very likely the structure of $Ag_{44}(SeR)_{30}$ as well. The slight red shift of the excitations as compared to the thiolate cluster can be understood as a size effect from a slightly larger total volume of the selenolate cluster, as most of the transitions involve not only metal core electrons but the pi-systems of the ligand layer as well, in analogy to the corresponding thiolate-stabilized cluster.[38]

In summary, we show the existence of an extremely stable silver cluster system protected with selenolate, $Ag_{44}(SePh)_{30}$. The UV−Vis spectrum of this compound is almost identical to the recently (structurally) solved $Ag_{44}(SR)_{30}$, and TDDFT computations assuming the structure of the thiolate cluster reproduce the experimental UV−Vis data accurately. The stability of the cluster arising from the closed shell 18-electron system and structurally stable Keplerate core is clear from the electronic structure calculations. We believe that similarity of the $Ag_{44}(XR)_{30}$ (X = S, Se) system would lead to the exploration of properties of analogous metal nanosystems.

dx.doi.org/10.1021/jz401879c | J. Phys. Chem. Lett. 2013, 4, 3351−3355

EXPERIMENTAL METHODS

Materials used in the synthesis are listed in the Supporting Information.

1. Solid State Synthesis of Cluster 1. Initially, 23 mg of $AgNO_3$ (s) and 30 μL of benzeneselenol (l) were ground well in a clean agate mortar using a pestle. The color of the mixture changes to yellowish orange showing the formation of silver selenolate. To this mixture, 25 mg of solid $NaBH_4$ were added and the content was ground well until the color became dark yellow. Then, 5 mL of ethanol was added to the mixture and mixed well. Ethanol was added to wash out the extra ligand. The mixture was kept for 15−30 s until there was a color change from dark yellow to deep brown. The contents were then taken in a centrifuge tube and centrifuged at 3600 rpm for 4 min. The centrifugate was removed, and the residue was dissolved in acetone and again centrifuged for 3 min. The cluster, extracted in acetone, was collected and the residue was discarded. Deep pink colored Ag_{44} cluster was obtained in acetone and it was stored in a refrigerator at ∼4 °C. The percentage yield was 80%. Similarly, the Ag_{44} cluster can also be extracted in tetrahydrofuran (THF) and acetonitrile. In THF, it is comparatively less stable (stable up to 15 days) in contrast to acetonitrile and acetone (stable up to 2 months at ambient condition).

2. Solution Phase Synthesis of Cluster 1. This is a modified procedure of Bakr et al.,[40] where a two step synthesis route was followed. First, silver trifluoroacetate (15.78 mg, 0.0714 mmol) was dissolved in 7.2 mL acetonitrile and stirred for 5 min. Benzeneselenol (5 μL, 0.0471 mmol) was added to that solution and was left to stir for another 15 min (Solution A). In another conical flask, 28.6 mL acetonitrile solution of $NaBH_4$ (10.8 mg, 0.286 mmol) was kept for stirring for 30 min (Solution B). Then, Solution B was added to Solution A, and the reaction mixture was left to stir for 3 h at room temperature. The deep pink colored cluster was formed after 3 h and it was stored in refrigerator at ∼4 °C.

Computational methods are presented in the Supporting Information.

ASSOCIATED CONTENT

Supporting Information

Details of experimental procedures, instrumentation, description of the computational methods, photographs during synthesis, ^{1}HNMR, SEM/EDAX, XPS, comparative UV/Vis spectra prepared by solid & solution state routes, time dependent spectra and the analysis of the electronic structure of cluster **1**. This material is available free of charge via the Internet at http://pubs.acs.org.

AUTHOR INFORMATION

Corresponding Authors

*Fax: + 91-44 2257-0545; E-mail: pradeep@iitm.ac.in.

*E-mail: negishi@rs.kagu.tus.ac.jp.

Notes

The authors declare no competing financial interest.

ACKNOWLEDGMENTS

T.P. thanks the Department of Science and Technology (DST), Government of India, for constantly supporting his research program on nanomaterials. I.C. thanks IITM for research fellowships. Y.N. wishes to express his gratitude to the Toden foundation and Tokyo Ohka foundation for partial financial support. T.P. and H.H. acknowledge financial support from the bilateral Academy of Finland−DST India research program.

REFERENCES

(1) Brust, M.; Walker, M.; Bethell, D.; Schiffrin, D. J.; Whyman, R. Synthesis of Thiol-Derivatised Gold Nanoparticles in a Two-Phase Liquid−Liquid System. *J. Chem. Soc. Chem. Commun.* **1994**, *7*, 801−802.

(2) Brust, M.; Kiely, C. J. Some Recent Advances in Nanostructure Preparation from Gold and Silver Particles: A Short Topical Review. *Colloids Surf. A* **2002**, *202* (2−3), 175−186.

(3) Daniel, M.-C.; Astruc, D. Gold Nanoparticles: Assembly, Supramolecular Chemistry, Quantum-Size-Related Properties, and Applications toward Biology, Catalysis, and Nanotechnology. *Chem. Rev.* **2003**, *104* (1), 293−346.

(4) Eustis, S.; El-Sayed, M. A. Why Gold Nanoparticles Are More Precious than Pretty Gold: Noble Metal Surface Plasmon Resonance and Its Enhancement of the Radiative and Nonradiative Properties of Nanocrystals of Different Shapes. *Chem. Soc. Rev.* **2006**, *35* (3), 209−217.

(5) Jin, R. Quantum Sized, Thiolate-Protected Gold Nanoclusters. *Nanoscale* **2010**, *2* (3), 343−362.

(6) Wilcoxon, J. P.; Abrams, B. L. Synthesis, Structure and Properties of Metal Nanoclusters. *Chem. Soc. Rev.* **2006**, *35* (11), 1162−1194.

(7) Diez, I.; Ras, R. H. A. Fluorescent Silver Nanoclusters. *Nanoscale* **2011**, *3* (5), 1963−1970.

(8) Parker, J. F.; Fields-Zinna, C. A.; Murray, R. W. The Story of a Monodisperse Gold Nanoparticle: $Au_{25}L_{18}$. *Acc. Chem. Res.* **2010**, *43* (9), 1289−1296.

(9) Xie, J.; Zheng, Y.; Ying, J. Y. Protein-Directed Synthesis of Highly Fluorescent Gold Nanoclusters. *J. Am. Chem. Soc.* **2009**, *131* (3), 888−889.

(10) Choi, S.; Dickson, R. M.; Yu, J. Developing Luminescent Silver Nanodots for Biological Applications. *Chem. Soc. Rev.* **2012**, *41* (5), 1867−1891.

(11) Muhammed, M. A. H.; Verma, P. K.; Pal, S. K.; Kumar, R. C. A.; Paul, S.; Omkumar, R. V.; Pradeep, T. Bright, NIR-Emitting Au_{23} from Au_{25}: Characterization and Applications Including Biolabeling. *Chem.—Eur. J.* **2009**, *15* (39), 10110−10120.

(12) Chakraborty, I.; Bag, S.; Landman, U.; Pradeep, T. Atomically Precise Silver Clusters as New SERS Substrates. *J. Phys. Chem. Lett.* **2013**, *4* (16), 2769−2773.

(13) Chaudhari, K.; Xavier, P. L.; Pradeep, T. Understanding the Evolution of Luminescent Gold Quantum Clusters in Protein Templates. *ACS Nano* **2011**, *5* (11), 8816−27.

(14) Habeeb Muhammed, M. A.; Verma, P. K.; Pal, S. K.; Retnakumari, A.; Koyakutty, M.; Nair, S.; Pradeep, T. Luminescent Quantum Clusters of Gold in Bulk by Albumin-Induced Core Etching of Nanoparticles: Metal Ion Sensing, Metal-Enhanced Luminescence, and Biolabeling. *Chem.—Eur. J.* **2010**, *16* (33), 10103−10112.

(15) Udaya Bhaskara Rao, T.; Pradeep, T. Luminescent Ag_7 and Ag_8 Clusters by Interfacial Synthesis. *Angew. Chem., Int. Ed.* **2010**, *49* (23), 3925−3929.

(16) Xavier, P. L.; Chaudhari, K.; Baksi, A.; Pradeep, T. Protein-Protected Luminescent Noble Metal Quantum Clusters: An Emerging Trend in Atomic Cluster Nanoscience. *Nano Rev.* **2012**, *3*, 14767.

(17) Kimura, K.; Sugimoto, N.; Sato, S.; Yao, H.; Negishi, Y.; Tsukuda, T. Size Determination of Gold Clusters by Polyacrylamide Gel Electrophoresis in a Large Cluster Region. *J. Phys. Chem. C* **2009**, *113* (32), 14076−14082.

(18) Cathcart, N.; Mistry, P.; Makra, C.; Pietrobon, B.; Coombs, N.; Jelokhani-Niaraki, M.; Kitaev, V. Chiral Thiol-Stabilized Silver Nanoclusters with Well-Resolved Optical Transitions Synthesized by a Facile Etching Procedure in Aqueous Solutions. *Langmuir* **2009**, *25*, 5840−5846.

(19) Udayabhaskararao, T.; Pradeep, T. New Protocols for the Synthesis of Stable Ag and Au Nanocluster Molecules. *J. Phys. Chem. Lett.* **2013**, *4* (9), 1553−1564.

(20) Bellon, P.; Manassero, M.; Sansoni, M. Crystal and Molecular Structure of Tri-iodoheptakis(tri-*p*-fluorophenylphosphine)-undecagold. *J. Chem. Soc., Dalton Trans.* **1972**, *14*, 1481−1487.
(21) Bellon, P. L.; Cariati, F.; Manassero, M.; Naldini, L.; Sansoni, M. Novel Gold Clusters. Preparation, Properties, and X-ray Structure Determination of Salts of Octakis(triarylphosphine)enneagold, $[Au_9L_8]X_3$. *J. Chem. Soc., D: Chem. Commun.* **1971**, *22*, 1423−1424.
(22) Schmid, G.; Pfeil, R.; Boese, R.; Bandermann, F.; Meyer, S.; Calis, G. H. M.; van der Velden, J. W. A. $Au_{55}[P(C_6H_5)_3]_{12}Cl_6$ — Ein Goldcluster Ungewöhnlicher Größe. *Chem. Ber.* **1981**, *114* (11), 3634−3642.
(23) Schmid, G. The Relevance of Shape and Size of Au_{55} Clusters. *Chem. Soc. Rev.* **2008**, *37* (9), 1909−1930.
(24) Bartlett, P. A.; Bauer, B.; Singer, S. J. Synthesis of Water-Soluble Undecagold Cluster Compounds of Potential Importance in Electron Microscopic and Other Studies of Biological Systems. *J. Am. Chem. Soc.* **1978**, *100* (16), 5085−5089.
(25) Heaven, M. W.; Dass, A.; White, P. S.; Holt, K. M.; Murray, R. W. Crystal Structure of the Gold Nanoparticle $[N(C_8H_{17})_4][Au_{25}(SCH_2CH_2Ph)_{18}]$. *J. Am. Chem. Soc.* **2008**, *130* (12), 3754−3755.
(26) Zhu, M.; Aikens, C. M.; Hollander, F. J.; Schatz, G. C.; Jin, R. Correlating the Crystal Structure of a Thiol-Protected Au_{25} Cluster and Optical Properties. *J. Am. Chem. Soc.* **2008**, *130* (18), 5883−5885.
(27) Qian, H.; Eckenhoff, W. T.; Zhu, Y.; Pintauer, T.; Jin, R. Total Structure Determination of Thiolate-Protected Au_{38} Nanoparticles. *J. Am. Chem. Soc.* **2010**, *132* (24), 8280−8281.
(28) Jadzinsky, P. D.; Calero, G.; Ackerson, C. J.; Bushnell, D. A.; Kornberg, R. D. Structure of a Thiol Monolayer-Protected Gold Nanoparticle at 1.1 Å Resolution. *Science* **2007**, *318* (5849), 430−433.
(29) Zeng, C.; Qian, H.; Li, T.; Li, G.; Rosi, N. L.; Yoon, B.; Barnett, R. N.; Whetten, R. L.; Landman, U.; Jin, R. Total Structure and Electronic Properties of the Gold Nanocrystal $Au_{36}(SR)_{24}$. *Angew. Chem., Int. Ed.* **2012**, *51* (52), 13114−13118.
(30) Zeng, C.; Li, T.; Das, A.; Rosi, N. L.; Jin, R. Chiral Structure of Thiolate-Protected 28-Gold-Atom Nanocluster Determined by X-ray Crystallography. *J. Am. Chem. Soc.* **2013**, *135*, 10011−10013.
(31) Yang, H.; Lei, J.; Wu, B.; Wang, Y.; Zhou, M.; Xia, A.; Zheng, L.; Zheng, N. Crystal Structure of a Luminescent Thiolated Ag Nanocluster with an Octahedral Ag_6^{4+} Core. *Chem. Commun.* **2013**, *49* (3), 300−302.
(32) Yang, H.; Wang, Y.; Zheng, N. Stabilizing Subnanometer Ag(0) Nanoclusters by Thiolate and Diphosphine Ligands and Their Crystal Structures. *Nanoscale* **2013**, *5* (7), 2674−2677.
(33) Bertorelle, F.; Hamouda, R.; Rayane, D.; Broyer, M.; Antoine, R.; Dugourd, P.; Gell, L.; Kulesza, A.; Mitric, R.; Bonacic-Koutecky, V. Synthesis, Characterization and Optical Properties of Low Nuclearity Liganded Silver Clusters: $Ag_{31}(SG)_{19}$ and $Ag_{15}(SG)_{11}$. *Nanoscale* **2013**, *5* (12), 5637−43.
(34) Guo, J.; Kumar, S.; Bolan, M.; Desireddy, A.; Bigioni, T. P.; Griffith, W. P. Mass Spectrometric Identification of Silver Nanoparticles: The Case of $Ag_{32}(SG)_{19}$. *Anal. Chem.* **2012**, *84* (12), 5304−8.
(35) Wu, Z.; Lanni, E.; Chen, W.; Bier, M. E.; Ly, D.; Jin, R. High Yield, Large Scale Synthesis of Thiolate-Protected Ag_7 Clusters. *J. Am. Chem. Soc.* **2009**, *131* (46), 16672−16674.
(36) Chakraborty, I.; Udayabhaskararao, T.; Pradeep, T. High Temperature Nucleation and Growth of Glutathione Protected ~ Ag_{75} Clusters. *Chem. Commun.* **2012**, *48* (54), 6788−6790.
(37) Desireddy, A.; Conn, B. E.; Guo, J.; Yoon, B.; Barnett, R. N.; Monahan, B. M.; Kirschbaum, K.; Griffith, W. P.; Whetten, R. L.; Landman, U.; Bigioni, T. P. Ultrastable Silver Nanoparticles. *Nature* **2013**, DOI: 10.1038/nature12523.
(38) Yang, H.; Wang, Y.; Huang, H.; Gell, L.; Lehtovaara, L.; Malola, S.; Häkkinen, H.; Zheng, N. All-Thiol-Stabilized Ag_{44} and $Au_{12}Ag_{32}$ Nanoparticles with Single-Crystal Structures. *Nat. Commun.* **2013**, DOI: 10.1038/ncomms3422.
(39) Lopez-Acevedo, O.; Akola, J.; Whetten, R. L.; Grönbeck, H.; Häkkinen, H. Structure and Bonding in the Ubiquitous Icosahedral Metallic Gold Cluster $Au_{144}(SR)_{60}$. *J. Phys. Chem. C* **2009**, *113* (13), 5035−5038.
(40) Chakraborty, I.; Govindarajan, A.; Erusappan, J.; Ghosh, A.; Pradeep, T.; Yoon, B.; Whetten, R. L.; Landman, U. The Superstable 25 kDa Monolayer Protected Silver Nanoparticle: Measurements and Interpretation as an Icosahedral $Ag_{152}(SCH_2CH_2Ph)_{60}$ Cluster. *Nano Lett.* **2012**, *12* (11), 5861−5866.
(41) Kurashige, W.; Yamaguchi, M.; Nobusada, K.; Negishi, Y. Ligand-Induced Stability of Gold Nanoclusters: Thiolate versus Selenolate. *J. Phys. Chem. Lett.* **2012**, *3* (18), 2649−2652.
(42) Kurashige, W.; Yamazoe, S.; Kanehira, K.; Tsukuda, T.; Negishi, Y. Selenolate-Protected Au_{38} Nanoclusters: Isolation and Structural Characterization. *J. Phys. Chem. Lett.* **2013**, 3181−3185.
(43) Negishi, Y.; Kurashige, W.; Kamimura, U. Isolation and Structural Characterization of an Octaneselenolate-Protected Au_{25} Cluster. *Langmuir* **2011**, *27* (20), 12289−12292.
(44) Xu, Q.; Wang, S.; Liu, Z.; Xu, G.; Meng, X.; Zhu, M. Synthesis of Selenolate-Protected $Au_{18}(SeC_6H_5)_{14}$ Nanoclusters. *Nanoscale* **2013**, *5* (3), 1176−82.
(45) Zaluzhna, O.; Zangmeister, C.; Tong, Y. J. Synthesis of Au and Ag Nanoparticles with Alkylselenocyanates. *RSC Adv.* **2012**, *2* (19), 7396−7399.
(46) AbdulHalim, L. G.; Ashraf, S.; Katsiev, K.; Kirmani, A. R.; Kothalawala, N.; Anjum, D. H.; Abbas, S.; Amassian, A.; Stellacci, F.; Dass, A.; Hussain, I.; Bakr, O. M. A Scalable Synthesis of Highly Stable and Water Dispersible $Ag_{44}(SR)_{30}$ Nanoclusters. *J. Mater. Chem. A* **2013**, *1*, 10148−10154.
(47) Bakr, O. M.; Amendola, V.; Aikens, C. M.; Wenseleers, W.; Li, R.; Dal Negro, L.; Schatz, G. C.; Stellacci, F. Silver Nanoparticles with Broad Multiband Linear Optical Absorption. *Angew. Chem.* **2009**, *121* (32), 6035−6040.
(48) Harkness, K. M.; Tang, Y.; Dass, A.; Pan, J.; Kothalawala, N.; Reddy, V. J.; Cliffel, D. E.; Demeler, B.; Stellacci, F.; Bakr, O. M.; McLean, J. A. $Ag_{44}(SR)_{30}^{4+}$: A Silver-Thiolate Superatom Complex. *Nanoscale* **2012**, *4* (14), 4269−4274.
(49) Rao, T. U. B.; Nataraju, B.; Pradeep, T. Ag_9 Quantum Cluster through a Solid-State Route. *J. Am. Chem. Soc.* **2010**, *132* (46), 16304−16307.
(50) Bootharaju, M. S.; Pradeep, T. Uptake of Toxic Metal Ions from Water by Naked and Monolayer Protected Silver Nanoparticles: An X-ray Photoelectron Spectroscopic Investigation. *J. Phys. Chem. C* **2010**, *114* (18), 8328−8336.
(51) Chakraborty, I.; Udayabhaskararao, T.; Pradeep, T. Luminescent Sub-nanometer Clusters for Metal Ion Sensing: A New Direction in Nanosensors. *J. Hazard. Mater.* **2012**, *211*, 396−403.
(52) Walter, M.; Akola, J.; Lopez-Acevedo, O.; Jadzinsky, P. D.; Calero, G.; Ackerson, C. J.; Whetten, R. L.; Grönbeck, H.; Häkkinen, H. A Unified View of Ligand-Protected Gold Clusters As Superatom Complexes. *Proc. Natl. Acad. Sci. U.S.A.* **2008**, *105* (27), 9157−9162.